through the 400-nm region.[15] This expected absorption at 395 and 415 nm will yield the resonance Raman effect necessary for detection. Strong lines near 1600 cm^{-1} would be expected for the system of a ring carbonyl conjugated with two carbon-carbon double bonds.[12,16] As previously mentioned, we do not think these strong lines represent the acetyl carbonyl modes.

The kinetic and structural usefulness of the transient Raman technique is shown by the following facts: (a) We actually resolve two additional intermediates I1 and I2, whereas the transient absorption in ethanol (figure 1 of reference 10) barely indicates a weak, broad spectrum near 315 nm on top of the phenoxy absorption. (b) An *intense* resonance Raman effect is not required to detect these species, as our probe laser wavelengths lie only in the weak tail of the apparent transient absorption. On the other hand, detection at these concentration levels does require at least a modest resonance Raman effect.

We speculate that I1 is the ortho, and I2 is the para, compound. I1 is the dominate intermediate and decays faster; ortho HoA is the dominante photoproduct. One might logically expect the ortho compound to unimolecularly decay into ortho HoA faster at neutral pH.

In the Table II the relative yields of I1 and I2 vs. phenoxy vary strongly with solvent. This result is as expected if the cyclohexadienones and free phenoxy radicals are competing products for caged radicals as in Scheme I. This result is consistent with the previously reported variation in final products, which has been used to support the solution phase, cage effect photo-Fries mechanism.[9,10]

Table II shows that the relative yields are not simply correlated with bulk solvent viscosity; the chemical and physical nature of the solvent molecules clearly affect the reaction. A specific comparison of the chemically similar molecules methanol and ethylene glycol shows that high viscosity strongly favors the recombination products I1 and I2. This is the expected cage effect behavior. However, CCl_4 has about the same viscosity as H_2O, and yet phenoxy is strongly favored in CCl_4. This may reflect the fact that acetyl radicals can abstract Cl atoms from CCl_4.[17] If Cl abstraction competes with caged radical recombination, then the I1 and I2 yields will be decreased. This mechanism, if correct, would provide direct experimental evidence against a concerted mechanism of I1 and I2 production.

Conclusions

(1) Transient spontaneous Raman spectroscopy shows the existence of three intermediate species formed via unimolecular photolysis of phenyl acetate. One species is the phenoxy radical, and the other two appear to be 6- and 4-acetylcyclohexadienones. (2) A strong solvent dependence in the relative yields of phenoxy vs. (apparently) cyclohexadienone intermediates supports the caged radical photo-Fries mechanism. The competitive yields of geminate recombination vs. radical escape do not correlate with bulk viscosity.

Acknowledgment. We thank H. Roth and M. Kaplan for useful discussions. We also thank T. Wolf for gas chromatography analyses.

Registry No. I1, 80753-89-5; **I2**, 80753-90-8; phenyl acetate, 122-79-2; phenol, 108-95-2; phenyl propionate, 637-27-4; phenoxy radical, 2122-46-5.

(15) G. Quinkert, *Angew. Chem., Int. Ed. Engl.*, **11**, 1073 (1972).
(16) For example, see Y. Nishimura and M. Tsuboi, "Proceedings of the International Conference on Raman Spectroscopy, 7th"; North Holland: Amsterdam, 1980, p 568.
(17) We thank Heinz Roth for this suggestion.

Model Calculations of Kinetic Isotope Effects for the Solvolysis of Neopentyl Arenesulfonates

Hiroshi Yamataka* and Takashi Ando*

Contribution from the Institute of Scientific and Industrial Research, Osaka University, Suita, Osaka 565, Japan. *Received June 26, 1981*

Abstract: Model calculations of α-^{14}C, β-^{14}C, γ-^{14}C, α-D_2, and γ-D_3 kinetic isotope effects in the acetolysis of neopentyl arenesulfonate were carried out for two possible pathways, concerted (k_Δ) and stepwise (k_c). In the k_Δ transition state (TS), four bond orders, $n_{\alpha-O}$, $n_{\alpha-\beta}$, $n_{\beta-\gamma}$, and $n_{\alpha-\gamma}$, were taken as independent parameters which define the model, whereas in the k_c model, $n_{\alpha-O}$, $n_{\alpha-\beta}$, $n_{\beta-\gamma}$, and $n_{\gamma-H}$ were taken as the parameters; other geometrical parameters and diagonal force constants were related to these four parameters by empirical expressions. One or more off-diagonal force constants were used to generate the reaction-coordinate frequency. The calculations suggested that the reaction proceeds via the k_Δ pathway whose TS has a weak but significant α-γ interaction; the alternative k_c pathway was shown to be less probable. The k_Δ TS structure determined was then compared with that of the 2-methyl-2-phenylpropyl (neophyl) solvolysis. The calculated k_Δ TS of the neopentyl solvolysis has (1) a stronger C_α-O bond, (2) a stronger C_α-C_β bond, (3) a weaker C_β-C_γ bond, and (4) a weaker C_α-C_γ bond than the TS of the neophyl solvolysis has. The results were interpreted in terms of the difference in the migrating group, methyl vs. phenyl, and it was concluded that the major mode of neighboring group participation by the phenyl is bridging whereas that by the methyl is hyperconjugation.

The mechanism of the neopentyl solvolysis (Scheme I) has been a subject of discussion for a long time, and various approaches have been tried in order to determine whether the mechanism is concerted (k_Δ) or stepwise (k_c).[1]

Quite recently, two groups reported the results of kinetic isotope-effect studies which provided strong support for the k_Δ mechanism.[2,3] Observations of normal carbon-14 isotope effects at the α-, β-, and γ-positions in the acetolysis of neopentyl nosylate (**1**, X = *p*-nitrobenzenesulfonate) indicated that the bondings at the three positions change in the transition state (TS). The results are consistent with the k_Δ pathway. Furthermore, the magnitudes

(1) For a recent review of the topic, see: Harris, J. M. *Prog. Phys. Org. Chem.* **1974**, *11*, 89-173.
(2) Ando, T.; Yamataka, H.; Morisaki, H.; Yamawaki, J.; Kuramochi, J.; Yukawa, Y. *J. Am. Chem. Soc.* **1981**, *103*, 430-436.
(3) Shiner, V. J., Jr.; Tai, J. J. *J. Am. Chem. Soc.* **1981**, *103*, 436-442.

0002-7863/82/1504-1808$01.25/0

Scheme I

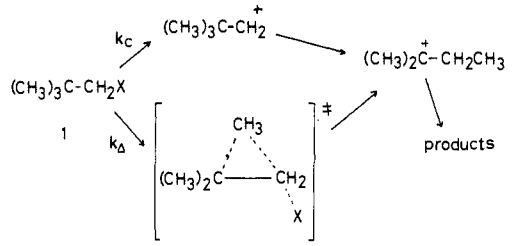

of these isotope effects were similar to those reported for the k_Δ solvolysis of 2-methyl-2-phenylpropyl (neophyl) ester (**2**) at each corresponding labeled position;[4]

$$\underset{\mathbf{2}}{C_6H_5(CH_3)_2CCH_2X}$$

this suggested that both reactions may proceed via the same mechanism, namely, k_Δ.

However, it should be noted that the isotope-effect results by themselves cannot completely eliminate the possibility that the reaction proceeds via the k_c pathway whose TS is stabilized by C_β–C_γ hyperconjugation. The bondings at all of the α-, β-, and γ-positions in such a TS may differ from those in the reactant, giving rise to the experimentally observed isotope effects.

These experimental isotope effects were expected to provide decisive information on the reaction mechanism when coupled with model calculations of the effects.[5] Kinetic isotope effects are calculated in terms of the expression of Bigeleisen and Mayer[6] from vibrational frequencies for both reactant and TS; the frequencies are obtained by vibrational analysis[7] for assumed geometries and force fields. If kinetic isotope effects are available at a number of different positions of a reactant, comparison of the calculated results with the experimental data allows quantitative discussion of the TS structure of the reaction. By this approach, the TS structures have been estimated for the solvolysis of *tert*-butyl chloride (S_N1),[8] elimination of (2-phenylethyl)trimethylammonium salt (E2),[9] and for the solvolysis of neophyl brosylate (**2**, X = *p*-bromobenzenesulfonate, k_Δ).[10]

In the present investigation, the model calculations of the isotope effects in the acetolysis of **1** were carried out for two possible pathways, k_Δ and k_c. Likely TS structures were determined by matching the calculated isotope effects with the experimental values. The most probable TS structure determined was then compared with that obtained previously for the acetolysis of **2**.[10]

Calculations

The calculation of isotope effects was carried out by use of program BEBOVIB-IV.[11] The program calculates molecular weight, principal moment of inertia, and vibrational frequencies for both the reactant and TS models and isotope effects from bonding parameters and force constants. The method used to construct the geometrical and the force field models are similar to those employed earlier for the k_Δ solvolysis of **2**.[10]

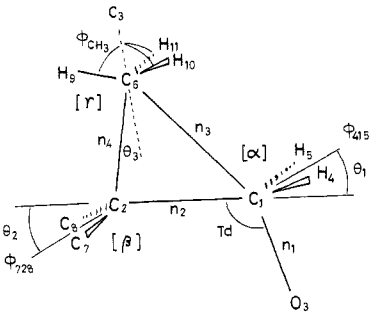

Figure 1. 11-atom cut-off model for reactant and TS.

Geometrical Models. The geometrical model employed for both the reactant and the TS was an 11-atom cut-off model (Figure 1) which contains a plane of symmetry defined by atoms C_1, C_2, O_3, C_6, and H_9. In the reactant model, tetrahedral geometry was assumed about the α, β, and γ-carbons (C_1, C_2, and C_6, respectively). All bond orders were assumed to be unity and their bond lengths to be the standard values r_0,[12] except for bond 3 which appears in the reactant model for the k_Δ pathway. The length of bond 3 was determined by the law of cosines using the two bond lengths, r_2 and r_4, and the angle ϕ_{126}. The order of bond 3 was calculated from its bond length by using the following revised version of Pauling's expression.[13]

$$r = r_0 - 0.3 \ln (n) \tag{1}$$

In the k_Δ TS, bond orders of the four reacting bonds, 1–4, were taken as independent parameters, and bond lengths of these bonds were adjusted by eq 1. All nonreacting bonds were assumed to have bond orders of unity as in the reactant. The angle to the leaving group (ϕ_{213}) was assumed to retain tetrahedral geometry during the reaction.[14] The bond angles within the cyclic moiety in the TS model (ϕ_{216}, ϕ_{126}, and ϕ_{162}) were determined by using the bond lengths r_2, r_3, and r_4. The other angles, ϕ_{415}, ϕ_{728}, θ_1, and θ_2, were calculated from the related bond orders by

$$\phi_{415} = 120.0 - 10.53|n_1 - n_3| \tag{2}$$

$$\phi_{728} = 120.0 - 10.53n_4 \tag{3}$$

$$\theta_1 = (\phi_{213}n_1 - \phi_{216}n_3)/(n_1 + n_2 + n_3) \tag{4}$$

$$\theta_2 = \phi_{126}n_4/(n_2 + n_4) \tag{5}$$

The angle θ_3 between the C_β–C_γ bond and the axis of the local C_3-type symmetry about C_γ and the angles ϕ_{CH_3} between the axis and each of the three C_γ–H bonds were adjusted by

$$\theta_3 = \phi_{162}n_3/(n_3 + n_4) \tag{6}$$

$$\phi_{CH_3} = 90.0 - 19.46(n_3 + n_4) \tag{7}$$

All these equations were designed to simulate the geometrical changes between the reactant and the TS consistent with the expected hybridization changes.

In the k_c TS model, no bond between C_α and C_γ was assumed, and the valence angle, C_α–C_β–C_γ, was retained constant at 109.5°. This assumption reduces the independent bonding parameters from four to three. Instead, the C_γ–H bond order ($n_{\gamma\text{-H}}$) was introduced as one of the parameters in the later part of the calculation.

(4) Yamataka, H.; Kim, S.-G.; Ando, T.; Yukawa, Y. *Tetrahedron Lett.* **1973**, 4767–4770.
(5) (a) Melander, L.; Saunders, W. H., Jr. "Reaction Rates of Isotopic Molecules"; Wiley-Interscience: New York, 1980. (b) Willi, A. V. In "Isotopes in Organic Chemistry"; Buncel, E.; Lee, C. C., Ed.; Elsevier: Amsterdam, 1977; Vol. III, Chapter 5.
(6) (a) Bigeleisen, J. *J. Chem. Phys.* **1949**, *17*, 675–678. (b) Bigeleisen, J.; Mayer, M. G. *Ibid.* **1947**, *15*, 261–267.
(7) Sellers, H. L.; Sims, L. B.; Schafer, L.; Lewis, D. E. *J. Mol. Struct.* **1977**, *41*, 149–151.
(8) Burton, G. W.; Sims, L. B.; Wilson, J. C.; Fry, A. *J. Am. Chem. Soc.* **1977**, *99*, 3371–3379.
(9) Lewis, D. E.; Sims, L. B.; Yamataka, H.; McKenna, J. *J. Am. Chem. Soc.* **1980**, *102*, 7411–7419.
(10) Ando, T.; Kim, S.-G.; Matsuda, K.; Yamataka, H.; Yukawa, Y.; Fry, A.; Lewis, D. E.; Sims, L. B.; Wilson, J. C. *J. Am. Chem. Soc.* **1981**, *103*, 3505–3516.
(11) Sims, L. B.; Burton, G. W.; Lewis, D. E. BEBOVIB-IV, Quantum Chemistry Program Exchange, No. 337, 1977.
(12) "Tables of Interatomic Distances and Configurations in Molecules and Ions"; The Chemical Society: London, 1958, 1965; Special Publications No. 11 and 18.
(13) Pauling, L. *J. Am. Chem. Soc.* **1947**, *69*, 542–553.
(14) One of the referees suggested that ϕ_{213} would not be constant at Td but expected to go to 90° as n_1 approaches zero. It is certain that ϕ_{213} is not constant during the course of the reaction, but there is no evidence that ϕ_{213} goes to 90°. At least in the region between the reactant and the TS, the tetrahedral angle seems to be a good approximation for ϕ_{213}. This is supported by our MO calculations (MINDO/3) for the k_Δ process of a neopentyl derivative in which the angle ϕ_{213} in the TS was calculated as 105.0°. Ando, T.; Yamataka, H.; Yabushita, S.; Yamaguchi, K.; Fueno, T. *Bull. Chem. Soc. Jpn.* **1981**, *54*, 3613–3614.

Table I. Structural Parameters[a] and Force Constants[b] for Reactant and Transition-State Models

bond stretch	reactant		transition state	
	r_i	F_{ii}	r_i	F_{ii}
C-C	1.537	4.5	$1.537 - 0.3 \ln(n)$	$4.5\ n_{C-C}$
C-O	1.43	5.3	$1.43 - 0.3 \ln(n)$	$5.3\ n_{C-O}$
C-H	1.094	5.0	$1.094 - 0.3 \ln(n)$	$5.0\ n_{C-H}$
angle bend	angle	F_α	angle	F_α
C-C-C	109.5	1.0	(c)	$1.0(n_{C-C}n_{C-C})^{1/2}g_\alpha$
H-C-O	109.5	0.75	(c)	$0.75(n_{C-O}n_{C-H})^{1/2}g_\alpha$
C-C-H	109.5	0.65	(c)	$0.65(n_{C-C}n_{C-H})^{1/2}g_\alpha$
H-C-H	109.5	0.55	(c)	$0.55(n_{C-H}n_{C-H})^{1/2}g_\alpha$

[a] Bond distances are given in angstroms and bond angles in degrees. [b] Stretching force constants are given in mdyn/Å and angle bending force constants in mdyn Å/rad². [c] See eq 2-7 of text.

Empirical equations employed to relate the TS geometry to the bonding parameters were the same as those for the k_Δ model (eq 1-7) except that n_3 was zero for the k_c model.

Force Field. A simple valence force field was used for both reactant and TS models except for one or more off-diagonal force constants used to generate an imaginary reaction-coordinate frequency (ν^*_L) in the TS. A stretching force constant for each reacting bond was calculated by the Pauling-Badger relation[15]

$$F_{ii} = n_i F_{ii}^0 \tag{8}$$

where n_i is the order of the bond i and F_{ii}^0 is the standard force constant[16] for the single bond i. Angle bending force constants were determined by

$$F_\alpha = g_\alpha (n_i n_j)^{1/2} F_\alpha^0 \tag{9}$$

where F_α^0 is the standard angle bending force constant[16] for the tetrahedral angle formed by the adjacent bonds i and j and g_α is a geometrical or hybridization factor[7] given by

$$g_\alpha = 1.39 + 1.17 \cos \alpha \tag{10}$$

Diagonal force constants used for both reactant and TS models are summarized in Table I.

Reaction-Coordinate Generation. One off-diagonal force constant, f_{13}, which couples the stretching modes of bonds 1 and 3 was used in the k_Δ TS model to generate an S_N2-like asymmetric reaction-coordinate motion at C_α. The magnitude of f_{13} was determined by

$$f_{13} = A(F_{11}F_{33})^{1/2} \tag{11}$$

where F_{11} and F_{33} are the stretching force constants of bonds 1 and 3, respectively, and A is a proportionality (interaction) constant. The reaction-coordinate motion for the k_c TS model was generated in two ways: (1) $F^*_{\alpha-O}$, the stretching force constant of the C_α-O bond in the TS, was set equal to zero or negative (e.g., -2.0), as is usually done for an S_N1,[7] or (2) three off-diagonal elements (those between $F^*_{\alpha-O}$ and $F^*_{\alpha-\beta}$, $F^*_{\alpha-\beta}$ and $F^*_{\beta-\gamma}$, and $F^*_{\alpha-O}$ and $F^*_{\beta-\gamma}$) were introduced in the F matrix so as to generate a reaction-coordinate motion expected for the TS stabilized by the C_β-C_γ hyperconjugation.

Results

Experimental isotope effects for five different atoms in the acetolysis of **1** are listed in Table II. Data at the γ-position are those of 2-methyl-2-adamantanemethyl brosylate, which is a model compound of neopentyl esters designed to give the isotope effects of only the migrating methyl group.[2]

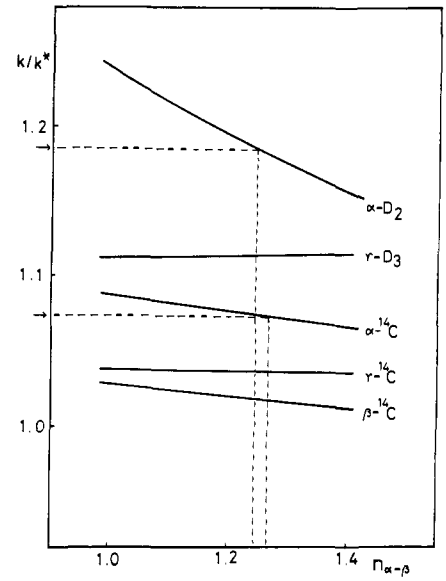

Figure 2. Calculated kinetic isotope effects vs. $n_{\alpha-\beta}$. $n_{\alpha-O} = 0.28$, $n_{\alpha-\gamma} = 0.05$, $n_{\beta-\gamma} = 0.67$, and $A = 1.50$. Arrows on the ordinate show the observed values of α-^{14}C (1.074) and α-D_2 (1.187) isotope effects.

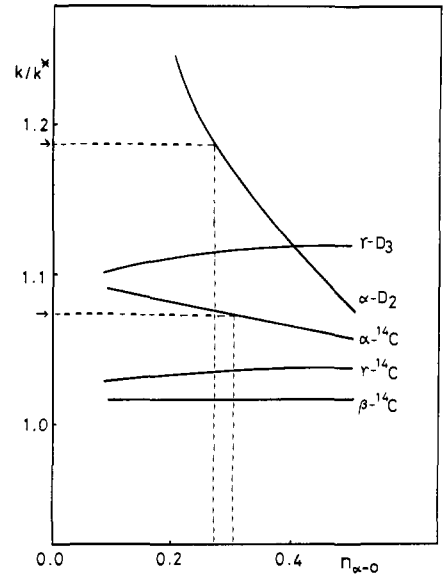

Figure 3. Calculated kinetic isotope effects vs. $n_{\alpha-O}$. $n_{\alpha-\beta} = 1.25$, $n_{\alpha-\gamma} = 0.05$, $n_{\beta-\gamma} = 0.67$, and $A = 1.50$. Arrows on the ordinate show the observed values of α-^{14}C (1.074) and α-D_2 (1.187) isotope effects.

In the k_Δ model, there are five independent parameters to be determined: four bond orders, $n_{\alpha-O}$ (or n_1), $n_{\alpha-\beta}$ (or n_2), $n_{\alpha-\gamma}$ (or n_3), and $n_{\beta-\gamma}$ (or n_4), used to construct the geometry, and one interaction constant, A, used to generate the reaction-coordinate frequency. Figure 2 shows the calculated isotope effects as functions of $n_{\alpha-\beta}$. It can be seen that the magnitudes of the isotope effects at the γ-position are essentially independent of $n_{\alpha-\beta}$. Similarly, as can be seen from Figure 3, the magnitudes of the γ-^{14}C, γ-D_3, and β-^{14}C isotope effects are relatively insensitive to $n_{\alpha-O}$. These results indicate that both carbon and deuterium isotope effects at the γ-position depend mainly on the two bonding parameters, $n_{\alpha-\gamma}$ and $n_{\beta-\gamma}$, for a given value of A. Therefore, the contour map of the two isotope effects can be drawn on a plane defined by $n_{\alpha-\gamma}$ (abscissa) and $n_{\beta-\gamma}$ (ordinate) as shown in Figure 4, where the lower left-hand corner corresponds to the reactant, and the upper right-hand corner to the tertiary carbocation intermediate. Solid and dashed lines are the constant isotope-effect curves for γ-^{14}C and γ-D_3, respectively. It is clear from the contour map (see circle) that in order to reproduce the two isotope effects at the γ-position simultaneously in the case of $A = 1.5$,

(15) Johnston, H. S. "Gas Phase Reaction Rate Theory"; Ronald Press: New York, 1966; pp 72-83.

(16) (a) Wilson, E. B., Jr.; Decius, J. C.; Cross, P. C. "Molecular Vibration"; McGraw-Hill: New York, 1955; pp 175-176. (b) Herzberg, G. "Infrared and Raman Spectra"; Van Nostrand: Princeton, NJ, 1945. (c) Schachtschneider, J. H.; Snyder, R. G. *Spectrochim. Acta* **1963**, *19*, 117-168. Snyder, R. G.; Schachtschneider, J. H. *Ibid.* **1965**, *21*, 169-195; *J. Mol. Spectrosc.* **1969**, *30*, 290-309.

Table II. Experimental Isotope Effects[a] and Calculated Kinetic Isotope Effects for the k_Δ and the k_c TS Models[b] in the Acetolysis of Neopentyl Nosylate at 100 °C

		k_Δ TS model			k_c TS model		
	exptl KIE	TDF	TIF	KIE	TDF	TIF	KIE
α-^{14}C	1.074 ± 0.002	1.047	1.026	1.074 (35.5)	1.046	1.027	1.074 (37.3)
β-^{14}C	1.019 ± 0.002	1.007	1.012	1.020 (63.9)	1.015	1.003	1.018 (18.3)
γ-^{14}C	1.037[c] ± 0.003	1.016	1.020	1.037 (56.1)	1.036	1.001	1.038 (3.2)
α-D_2	1.187 ± 0.001	1.159	1.026	1.188 (14.8)	1.146	1.034	1.186 (19.8)
γ-D_3	1.123[c] ± 0.002	1.080	1.039	1.122 (32.9)	1.118	1.004	1.122 (3.4)

[a] Reference 2. [b] KIE is an overall kinetic isotope effect; for TDF and TIF see eq 12 of text. Figures in parentheses show the percent contributions of TIF to KIE. [c] Values for the migrating methyl group in the acetolysis of 2-methyl-2-adamantanemethyl brosylate.

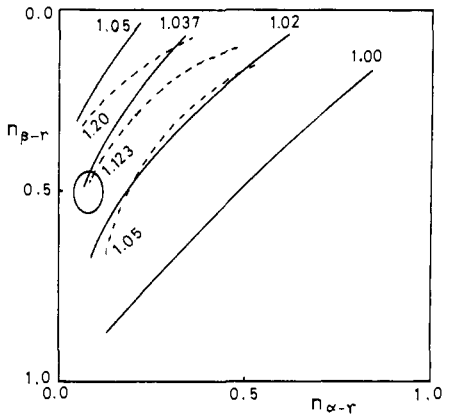

Figure 4. Constant isotope effect curves for γ-^{14}C (solid curve) and γ-D_3 (dashed curve) isotope effects. $n_{\alpha-\beta} = 1.20$, $n_{\alpha-O} = 0.05$, and $A = 1.50$. A circle in the figure shows the region where the two constant isotope effect curves (γ-^{14}C, 1.037; γ-D_3, 1.123) may intersect.

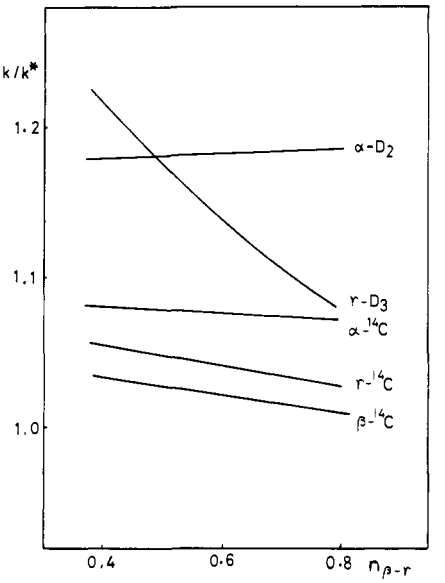

Figure 5. Calculated kinetic isotope effects vs. $n_{\beta-\gamma}$. $n_{\alpha-O} = 0.28$, $n_{\alpha-\beta} = 1.25$, $n_{\alpha-\gamma} = 0.05$, and $A = 1.50$.

$n_{\alpha-\gamma}$ must be very small and $n_{\beta-\gamma}$ must be about one-half its reactant value.[17]

On the other hand, the carbon and deuterium isotope effects at the α-position are insensitive to $n_{\beta-\gamma}$, as shown in Figure 5, but their magnitudes depend on the other three bond orders, $n_{\alpha-\beta}$ (Figure 2), $n_{\alpha-O}$ (Figure 3), and $n_{\alpha-\gamma}$. Thus, with the value of $n_{\alpha-\gamma}$ obtained above, $n_{\alpha-\beta}$ and $n_{\alpha-O}$ can be determined by matching the two isotope effects, α-^{14}C and α-D_2, with the experimental results. As Figures 2 and 3 show, the C_α–C_β bond must be stronger ($n_{\alpha-\beta} \sim 1.25$) than that of the reactant and the C_α–O bond must be largely broken ($n_{\alpha-O} \sim 0.3$) in the TS model for simultaneous reproduction of α-^{14}C and α-D_2 isotope effects.

Starting with these four bond orders roughly estimated above, the TS model was further refined so as to give the best reproduction of all five isotope effects simultaneously. The TS structure thus determined is shown in Figure 6a, and the calculated isotope effects are listed in Table II. Figure 6a also shows the reaction-coordinate motion in the TS, which is reasonable as that for the k_Δ TS. The reaction-coordinate frequency obtained was 184*i* cm^{-1}. It should be pointed out that slightly different structures were obtained depending on the *A* value used ($1.0 \le A \le 2.0$), but the differences were small. The final bond orders fell into the following ranges: $0.22 \le n_{\alpha-O} \le 0.28$, $0.048 \le n_{\alpha-\gamma} \le 0.074$, $0.63 \le n_{\beta-\gamma} \le 0.67$, and $n_{\alpha-\beta} = 1.25$.

In contrast to the case of the k_Δ model, reproduction of the experimental isotope effects by the k_c model was not straightforward. In particular, the two isotope effects at the γ-position were impossible to reproduce simultaneously with the three bonding parameters, $n_{\alpha-O}$, $n_{\alpha-\beta}$, and $n_{\beta-\gamma}$. Therefore, the bond order, $n_{\gamma-H}$, was introduced as an additional independent bonding parameter in the latter part of the calculations. This parameter allowed the TS to have a stronger C_γ–H bond when C_γ had a more sp^2 character. By adjusting these four bonding parameters, as well as a set of interaction constants, a family of TS structures was obtained which reproduced the five experimental isotope effects simultaneously. Although the structures differ slightly from each other depending on the magnitudes of the interaction constants used, they have the following common characteristics: (1) the C_β–C_γ bond is weakened to less than one-half its reactant value ($n_{\beta-\gamma} \sim 0.4$), (2) the C_γ–H bonds are slightly strengthened ($n_{\gamma-H} \sim 1.04$), and (3) the C_α–C_β bond is strengthened to a great extent ($n_{\alpha-\beta} \sim 1.6$) which completely compensates for the bonding loss at C_β caused by the C_β–C_γ bond weakening. The representative k_c TS structure is shown in Figure 6b together with its reaction-coordinate motion.

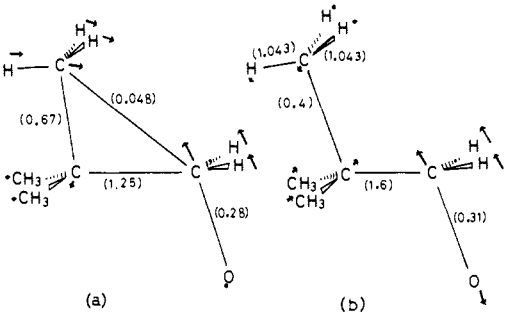

Figure 6. The final TS structures for the acetolysis of neopentyl nosylate. The reaction-coordinate motions are shown by arrows. Figures in parentheses are bond orders. (a) k_Δ TS model. (b) k_c TS model.

Discussion

The model calculations yielded two distinct TS models, one for the k_Δ pathway and the other for the k_c pathway. As can be seen

(17) One might notice in Figure 4 that in spite of the expected contribution of the reaction-coordinate motion the carbon isotope effect is nil or even inverse if the sum of the two bond orders ($n_{\alpha-\gamma} + n_{\beta-\gamma}$) is unity. The results are related to the fact that for these tentative models in which $n_{\alpha-\beta} = 1.20$ and $n_{\alpha-O} = 0.05$, the reaction coordinate is essentially the C_α–O bond cleavage. Since the migrating γ carbon participates little in the reaction-coordinate motion in these TS, the contribution of the motion to the γ-^{14}C isotope effect is negligible. The situation is similar to a very late TS of a bimolecular substitution, X + YZ → [X···Y···Z]* → XY + Z, in which the reaction coordinate is mainly dissociation of XY and Z. See: Buddenbaum, W. E.; Shiner, V. J., Jr. *Can. J. Chem.* **1976**, *54*, 1146–1161.

Scheme II

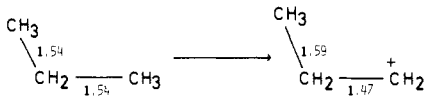

from Figure 6, the C_α–C_β and C_β–C_γ bond orders are changed considerably from their reactant values in both TS models. Thus, both models are consistent with the earlier qualitative conclusion that the three carbons, C_α, C_β, and C_γ, change their bondings in the TS.[2] However, there are two major differences between the models. First, the C_α–C_β bond in the k_c TS model is much stronger than the corresponding bond in the k_Δ model, and conversely the C_β–C_γ bond in the former is much weaker than the bond in the latter. Second, the reaction-coordinate motion in the k_c model is localized at the C_α–O bond cleavage, whereas the C_α–O bond cleavage and the C_α–C_γ bond formation are coupled in the k_Δ model.

According to Bigeleisen's formulation[18] (eq 12), kinetic isotope effects can be divided into two terms:

$$k_l/k_2 = [\nu^*_{1L}/\nu^*_{2L}][(VP)(EXC)(ZPE)]$$
$$= [\text{temperature-independent factor (TIF)}]$$
$$\times [\text{temperature-dependent factor (TDF)}] \quad (12)$$

The first one is the contribution from an imaginary reaction-coordinate frequency (TIF) and the second one is that from normal vibrations consisting of vibrational product, excitation, and zero-point energy factors (TDF). Table II lists the magnitudes of these terms for each isotope effect in both TS models. Marked differences are apparent in the TIF contributions which are shown in parentheses. For example, the contribution for the γ-^{14}C isotope effect is 56% in the k_Δ model while it is only 3% in the k_c model. It should be noted that these figures are the quantitative expression of the arrows in Figure 6. The large TIF of the γ-^{14}C isotope effect in the k_Δ model is consistent with the concerted nature of the k_Δ process. Thus, it is concluded that there is a good possibility of the solvolysis of **1** proceeding via the k_Δ process, whose TS structure is represented by the diagram in Figure 6a. The geometrical features of the TS, such as the small extent of the C_α–C_γ bond formation, are acceptable for the process and will be compared later with the TS structure of the k_Δ solvolysis of **2**.

In the k_c model, the negligible TIF contribution to the γ-^{14}C isotope effect is also consistent with the nature of the assumed k_c (simple ionization) process. However, the geometrical features, such as the very weak C_β–C_γ bond and the high double-bond character of the C_α–C_β bond, seem unreasonable for the k_c process, as discussed below.

First, if we assume that the C_α–O partial bond cleavage (0.69 bond order unit) gives rise to 0.69 unit of negative charge on the leaving group and the same amount of positive charge on the neopentyl moiety and that this positive charge is dispersed within the neopentyl moiety according to the loss of the total bond order at each position, it is computed that C_α, C_β, and the γ-methyl group are positively charged by 0.09, 0.0, and 0.6 unit, respectively. This means that 87% of the total positive charge is localized on the γ-methyl while only 13% is on the α-carbon. This charge distribution seems unlikely for a TS leading to the primary neopentyl cation. These figures rather remind us of a concerted fragmentation reaction, which actually does not occur.

Ab initio molecular orbital calculations provide another criterion of whether the model is suitable for the TS of the k_c process. Pople et al. calculated the structure of methyl-staggered 1-propyl cation stabilized by C–C hyperconjugation as well as the structure of propane (STO-3G level).[19] According to these calculations, both C_α–C_β and C_β–C_γ bond lengths of the 1-propyl cation differ only slightly from the C–C bond of propane, as is shown in Scheme II. In contrast, as shown in Scheme III, the C_β–C_γ bond of the

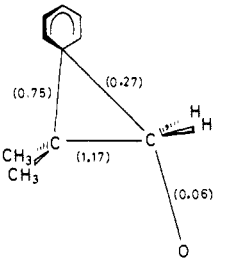

Figure 7. Final TS structure for the acetolysis of neophyl brosylate. Figures in parentheses are bond orders.

Scheme III

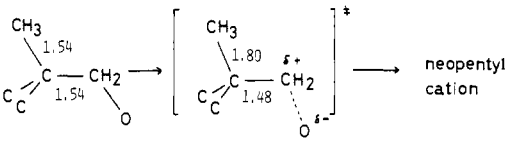

TS determined by the present model calculations is much longer than the bond of the reactant neopentyl ester, while the C_α–C_β bond of the TS is slightly shorter than the bond of the ester. If we assume that the two C–C bond lengths of the primary neopentyl cation in Scheme III are not much different from those of the propyl cation in Scheme II, the C_β–C_γ bond of the TS determined by the model calculations seems too long. This seems to eliminate the k_c process as a possibility.[20] In conclusion, the present study indicates that the actual solvolysis of **1** does not proceed via the k_c process but via the k_Δ process.

It is interesting to note here that as can be seen from Table II the γ-D_3 isotope effect in the k_Δ TS is caused mainly by the bonding changes such as the weakening of the C_β–C_γ bond and the contribution of the reaction-coordinate motion is subsidiary. This contrasts with the case of the γ-^{14}C isotope effect, in which the reaction-coordinate motion is a primary contributor. These results are consistent with the idea that the γ-D_3 isotope effect is of secondary type while the γ-^{14}C isotope effect is of primary type. Note also that the β-^{14}C isotope effect is caused primarily by the reaction-coordinate motion.

Although the k_Δ TS structure in Figure 6a may not be final in the sense that slightly different results may be obtained by use of model calculations based on different assumptions,[21] it is informative to compare the present results with those for a related reaction system obtained by the same calculation method. The usefulness of this type of comparison has been pointed out by Willi and Won,[22] who stated that calculated force constants "are certainly useful as relative parameters which give a qualitative description of a TS property, provided the calculation procedure and the force constant definitions are the same in all calculations".

We have previously reported the results of the same type of model calculations for the acetolysis of neophyl brosylate, **2**, whose TS structure is given in Figure 7.[10] Several differences are apparent between this and the TS structure of the acetolysis of neopentyl nosylate, **1**: the TS of acetolysis of **1** has (1) a stronger C_α–O bond, (2) a stronger C_α–C_β bond, (3) a weaker C_β–C_γ bond, and (4) a weaker C_α–C_γ bond than the TS of the acetolysis of **2** has. Since the difference in the leaving group (nosylate or

(18) Bigeleisen, J. *J. Chem. Phys.* **1949**, *17*, 675–678.

(19) (a) Radom, L.; Lathan, W. A.; Hehre, W. J.; Pople, J. A. *J. Am. Chem. Soc.* **1971**, *93*, 5339–5342; (b) Radom, L.; Pople, J. A.; Buss, V.; Schleyer, P. v. R. *Ibid.* **1972**, *94*, 311–321.

(20) Ab initio MO calculations at a higher level of approximation may give different structures, especially for 1-propyl cation, and model calculations of isotope effects based on different assumptions may give different TS models. We believe, however, that the structure of the TS determined by the present model calculations is so different from that of the 1-propyl cation determined by the MO method that our conclusion is correct, at least qualitatively.

(21) Two major simplifying assumptions were made in the model calculations. One is the empirical expressions employed to relate diagonal force constants to bond orders (eq 8 and 9 of text). The other is concerned with the treatment of off-diagonal force constants; most of the off-diagonal terms in the transition-state force-constant matrix as well as all of the terms in the reactant matrix were set to be zero. These assumptions are not considered to lead to serious problems judging from the reported success of this type of model calculations.[5,8-10]

(22) Willi, A. V.; Won, C. M. *J. Am. Chem. Soc.* **1968**, *90*, 5999–6001.

brosylate) seems not to influence the isotope effects much,[2] the results may be attributed mainly to the difference in the participating group, methyl or phenyl.

In the case of **2**, moderately nucleophilic π electrons of the phenyl ring can interact directly with the α carbon displacing the leaving group oxygen; in the TS, the phenyl ring participates mainly via 1,3 through-space interaction (reflected in a stronger C_α–C_γ bond). On the other hand, since no mobile π electrons are available for **1**, less nucleophilic σ electrons of the C_β–C_γ bond should interact with the α carbon (weak C_β–C_γ bond), and the interaction in this case occurs predominantly through the C_α–C_β bond (stronger C_α–C_β bond). Thus it can be concluded that the major mode of the participation by the phenyl ring is bridging whereas that by the methyl group is hyperconjugation. Although no calculations have been carried out for solvolysis with participation by the most nucleophilic lone-pair electrons (n participation), it can be reasonably expected that the 1,3 interaction is even stronger in the TS with n participation than that with π participation and that the relative importance of bridging over hyperconjugation increases from σ to n through π participation, constituting a sort of spectrum.

Acknowledgment. All calculations were performed by using the ACOS 900 computer at the Osaka University Computation Center. The present work was partly supported by a Grant-in-Aid for Science Research 347018 from the Ministry of Education, Science and Culture, Japan.

Registry No. 1 (X = *p*-nitrobenzenesulfonate), 13372-31-1.

Relative Bond Dissociation Energies for Two-Ligand Complexes of Ni^+ with Organic Molecules in the Gas Phase

Manfred M. Kappes[1a] and Ralph H. Staley*[1b]

Contribution from the Department of Chemistry, Massachusetts Institute of Technology, Cambridge, Massachusetts 02139. *Received July 29, 1981*

Abstract: Relative two-ligand dissociation enthalpies, $\delta D(Ni^+–2L)$, for Ni^+ with 50 organic molecules are determined. A pulsed laser volatilization–ionization source is used to generate Ni^+ which can react with various neutrals to give $Ni(ligand)_2^+$ species. Equilibrium constants are measured for the ligand-exchange reactions which occur when pairs of ligand molecules are present. Free energies for two-ligand exchange are obtained from the equilibrium constant for the reaction $Ni(A)_2^+ + 2B \rightleftarrows Ni(B)_2^+ + 2A$. The free-energy differences are added to give a scale of relative free energies for ligand exchange. These are converted to enthalpies to give $\delta D(Ni^+–2L)$. Dependence of $\delta D(Ni^+–2L)$ on functional groups and substituent effects is analyzed. The results for Ni^+ are compared to available results for other reference acids: H^+, Al^+, Mn^+, NO^+, Li^+, Co^+, Cu^+, and $CpNi^+$. The extensive data set for Ni^+ makes possible correlations which clearly demonstrate differences in bonding among different compound classes, in particular between oxygen compounds and alkenes, nitriles, sulfur bases, and other ligands capable of π-back-bonding. These comparisons show that Ni^+ is a substantially softer acid than NO^+, Li^+, Al^+, and H^+, slightly softer than Co^+ and $CpNi^+$, and slightly harder than Cu^+. The relative slopes of the correlation plots suggest that the average metal–ligand bonding distance for $Ni(ligand)_2^+$ complexes is shorter than that for both Co^+ and Cu^+.

Ion cyclotron resonance (ICR) spectroscopy with a pulsed-laser volatilization–ionization source of atomic metal cations has recently been applied to measure relative gas-phase ligand-binding energies for various metal cations. One-ligand binding energies, $D(M^+–L)$, were obtained for Al^+ and Mn^+[2,3] while two-ligand binding energies, $D(M^+–2L)$, were measured for Cu^+ and Co^+.[4,5] These binding energies, which are essentially basicities with the metal cation as reference acid, are useful in evaluating the energetics of reaction processes and in developing models for understanding molecular interactions. In addition, comparisons between different scales can be quite informative and often reveal interesting points about metal–ligand interactions. In particular, correlations of the previously measured data sets for Al^+, Mn^+, Cu^+, and Co^+ have provided quantitative measures of hard and soft acid base concepts unencumbered by solvation and other complicating effects.[4,5] Ideally, basicity scales should be determined for the same set of ligands. The resulting comparisons would then have complete overlap of data. Normally, due to experimental constraints, data overlap is less than ideal and in some cases quite poor. As a result, comparisons among the previously determined data sets are often not totally satisfying in that they suggest the occurrence of interesting systematic effects while not providing sufficient evidence for them. For example, the data suggest that in a given correlation plot, molecules of different functional groups may in general fall on different lines.[2–5] Usually the lines obtained for various oxygen functionalities are not distinguishable. Data points for cyanides, amines, sulfur compounds, and alkenes generally deviate quite appreciably from the line for oxygen bases and appear to fall on lines of their own. With minor exceptions, however, the data sets in previous studies have been inadequate to show whether the data for each of these other functionalities do indeed fall on separate lines.

In the present paper we report determinations of relative binding energies of 50 organic molecules in two-ligand complexes with Ni^+. The data set of ligands studied is much larger than in previous studies. The ligands measured were chosen to give as much overlap with other data sets as possible. In particular, the question of separate correlation lines for different functionalities was addressed by including appropriate cyanide, amine, sulfur base, and alkene molecules as ligands. The results are compared to available gas-phase basicity scales for the other reference acids: H^+, Li^+, NO^+, Al^+, Mn^+, Co^+, Cu^+, and $CpNi^+$ (Cp = η^5-C_5H_5).

Experimental Section

Experiments were carried out by using ICR instrumentation and techniques which have been previously described.[2–7] The output of a pulsed YAG laser is focused onto a nickel wire target at the end of the ICR cell to produce atomic nickel cations. The mass spectrum for this

(1) (a) Institute for Inorganic and Physical Chemistry, University of Bern, CH-3012 Bern, Switzerland; (b) Central Research Department, Experimental Station, DuPont Company, Wilmington, DE 19898.
(2) Uppal, J. S.; Staley, R. H. *J. Am. Chem. Soc.* **1982**, *104*, 1229, 1235.
(3) Uppal, J. S.; Staley, R. H. *J. Am. Chem. Soc.* **1982**, *104*, 1238.
(4) Jones, R. W.; Staley, R. H. *J. Am. Chem. Soc.*, submitted for publication.
(5) Jones, R. W.; Staley, R. H. *J. Am. Chem. Soc.*, submitted for publication.
(6) Jones, R. W.; Staley, R. H. *J. Am. Chem. Soc.* **1980**, *102*, 3794–3798.
(7) Uppal, J. S.; Staley, R. H. *J. Am. Chem. Soc.* **1980**, *102*, 4144–4149.

0002-7863/82/1504-1813$01.25/0